

Design of a Circular Micro-Strip Patch Antenna for Improved Directivity and Gain of Mobile Communication Base Station

Abstract

This study presents the design of Circular Micro-strip Patch Antenna (CMPA) for improved directivity and gain of mobile communication base station. The design incorporates a Rogger/5880 substrate material with a permittivity of 2.2, tangent angle of 0.00009 and a substrate height (thickness) of $0.98\mu\text{m}$ at a frequency of 1.65THz. Diversity Antenna Array Processing (DAAP) and Chebyshev Antenna Array (CAA) methods were used in the design. AutoCAD software and 2D data plotter were used for the diagrams and charts while Maple software was used for simulation. For angles of 0° , 30° , 60° , 90° , 120° , 150° and 180° , the array factors are 7.84dB, 7.85dB, 7.87dB, 7.88dB, 7.87dB, 7.85dB and 7.84db respectively. The results from the design demonstrated a remarkably low side lobe level of 0.01dB, indicating excellent suppression of unwanted radiation in undesired directions. Additionally, the antenna exhibits a Voltage Standing Wave Ratio (VSWR) of unity, ensuring maximum power transfer efficiency from the source to the load. Furthermore, the antenna shows a high directivity and gain of approximately 9dB, which enhances the signal strength and coverage range. The Half Power Beam-width (HPBW) and First Null Beam-width (FNBW) was measured as 30° and 60° respectively. These parameters depict the angular width of the main radiation beam and the sharpness of the beam pattern's nulls. In all, the designed CMPA with its CAA based antenna array holds great potential for communication networks and for mobile communication base station, offering enhanced performance in terms of radiation characteristics and signal quality.

Keywords: CMPA, AutoCAD,HPBW, FNBW, CAA, DAAP

1. Introduction

With the increasing demand for high-speed and reliable wireless communication, directional antenna systems have gained significant attention. This system utilizes antennadiversity transmission techniques. Using these techniques improves the signal quality by reducing interference, reducing multipath fading and it has become a popular approach for improving the performance of wireless networks/systems [1].

Recently, with the rapid development in telecommunication system, network providers are very much concerned about the limited capacity of their current networks [2]. The broad-spectrum call for data services, voice, personal, and visual enhancements have become larger than the available infrastructure. Greater numbers of subscribers around the world have no good interconnection mobile communication system activation even when the nation and network distributors have put in more effort to meet the global production needs. The biggest difficulty that countries and network operators face is the interconnectivity between subscribers and the widespread communication network and the usual conventional means of providing that relationship is complex and expensive [3]. They are also not sufficient to meet the data intensive implementation requirements. In this era of information technology, people are more interested in mobile/ wireless communication because with it people's lives can be positively affected [4]. The so-called line communication systems and coaxial cables have methodological difficulties. Despite the technical advantages of fiber optic cables and their widespread use in basic applications, installation costs are too high for home and market users. This is why wireless or free space access has significant advantage over fiber optic cables [5]. For this reason, wireless network is increasingly visualized as an unconventional alternative to quickly and inexpensively meeting flexible subscribers' interconnection requirements.

Advances in mobile/wireless technology and dramatic communication systems also show no signs of slowing down anytime soon. As technology advances, people's daily activities are being changed by the introduction of different technology and processes [6]. Radio frequency and mobile communication technology are now extensively utilized in both everyday human activities and various industrial sectors [7].

Also, as the demand for mobile communication is continuously growing, the need for better coverage, improved capacity and better transmission quality arises. The obvious issues that crop up are how to amass more capabilities so that a larger number of subscribers can be covered at reduced costs and maintaining the quality at the same time especially in areas where population is large. It also involves how to obtain significantly larger coverage to actually decrease maintenance and operation costs in areas where subscribers are relatively few in number. These challenges which are centered on the need for efficient use of the radio spectrum have spurred the adoption of intelligent directional antenna arrays around the world [8]. Due to the advancement in mobile communication innovations, the demand for communication equipment augments, having public mobile base

stations is requisite because base station antennas is vital for transmitting and receiving electromagnetic waves and also play an important role in antenna efficiency and communication quality stability [9].

Hence, this work seeks to design a Circular Micro-strip Patch Antenna (CMPA) for improved directivity and gain of mobile communication base station to enhance the overall system performance with respect to capacity, scope and service quality.

2. Materials and Method

2.1 Materials

In this study, the research method and parameters/materials employed in designing a circular micro-strip patch antenna is presented. This research work employs software tools like AutoCAD 2007 software and 2D data plotter for drawing diagrams and charts whereas Maple software was used for the simulation.

2.2 Method

2.2.1 System Design Methodology

Circular Micro-strip Patch Antenna for Mobile communication base Station operating at a frequency range of 300GHz to 3000GHz was considered in this work. Selection of elements that can conform to the geometry of the device and the array architecture that could control the radiation pattern both in azimuth and elevation directions was also considered. This resulted in the selection of micro-strip patches which are light in weight and low volume arranged in a planar configuration which can be easily made conformal to host surface [10].

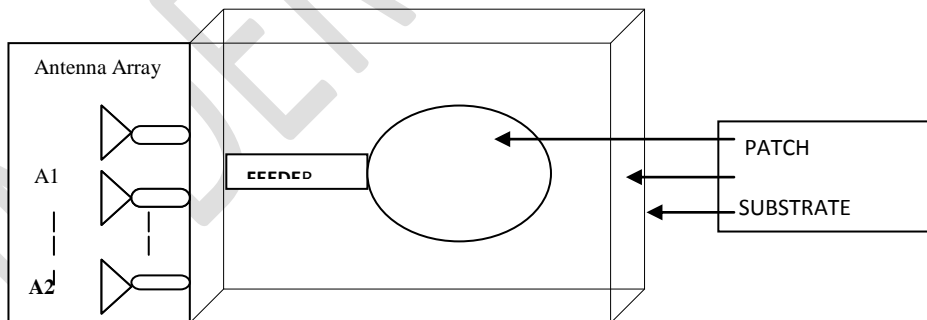


Fig. 1: Schematic diagram of Circular Micro-strip Patch Antenna (CMPA)

The architecture of the proposed Circular Micro-strip Patch Antenna (CMPA) system as shown in Fig.1. It consists of different parts, which are the metallic patch, the dielectric substrate, the feeder and the ground plane. Feeder is a pathway for the antenna array to the radiating patch and also excites the circular patch. It is typically

a micro-strip feed line that connects the circular patch to the external RF source or receiver. The patch is a conductive material (copper) placed on top of the dielectric substrate that radiate and receive electromagnetic waves with the antenna array which control the radiation pattern. The dielectric substrate is a non conductive material placed between the circular patch and the ground plane. It provides mechanical support and insulation between the conductive layers. The ground plane is a larger conductive plane usually copper placed on the bottom side of the dielectric substrate. Ground plane isolate stray radiation from the feed to achieve better radiation efficiency and performance [11]. It also acts as a reflector and provides a ground reference or return path for the antenna. The work goal is to design a Circular Micro-strip Patch Antenna (CMPA) for improved directivity and gain of communication base station to direct the beam towards the most pressing signal, thereby improving the coverage area, capacity, connectivity and effectiveness of the mobile communication system using diversity antenna array processing (DAAP) approach.

The CMPA operates by exciting the patch with Radio Frequency (RF) energy through the feed-line connecting the antenna array. When signal is applied to the patch, it creates an electric field across the patch surface. This electric field causes current to flow on the patch, generating electromagnetic waves. These waves radiate into free space, forming the designed radiation pattern that is determined by the antenna array, the patch design and the interaction with the ground plane.

2.2.2 Choice of Circular Micro-strip Patch Antenna

In this work, the type of antenna element considered is a Micro-strip patch antenna which is a type of antenna commonly used in wireless communication systems and is intended to be mounted on a smooth surface or similar device [10]. It consists of three layers structure, a radiating patch on one side of a dielectric substrate, with a ground plane on the other side [12]. The patch is typically made of conductive material like copper and is designed to radiate electromagnetic waves. Micro-strip patch antennas are popularly used in numerous applications due to their low profile, lightweight, and low cost of manufacturing [12]. Compared to the convectional antennas, the study of micro-strip patch antenna has made great progress in recent years [7]. Micro-patch antennas serve as high gain antennas suitable for low profile mobile applications operating at frequencies surpassing 100MHz [13]. This type of antenna have different shapes like circular, rectangular, elliptical, triangular and square but the rectangular, square and circular shapes are mostly used due to their simple design and performance analysis [14]. The circular shaped micro-strip patch antenna is better due to its design simplicity and their radiation pattern can be controlled. Also, the circular micro-strip patch antenna is

sixteen percent smaller than the rectangular micro-strip patch antenna designed for the same frequency range. Designing micro-strip patch antennas involves considerations such as the dimensions of the patch, the substrate material, the feed mechanism/technique, and the shape of the patch which can be circular, rectangular or other shapes. These factors affect the antenna's performance in terms of frequency, bandwidth, radiation pattern, and efficiency. Because circular micro-strip patch antenna have smaller size, offers higher bandwidth and less side lobe power than rectangular patch antenna, hence the choice of circular patch micro-strip antenna.

2.2.3 Design of Circular Micro-strip Patch Antenna (CMPA) for Terahertz Range

Circular micro-strip patch antenna is a piece of conductive material inscribed on a dielectric substrate. Dielectric material with low dielectric constant was selected to achieve higher efficiency and wider bandwidth. For the design of the micro-strip antenna, AutoCAD software, version 2007 was used. The Software is computer aided design (CAD) software that is widely used to create precise and high quality 2D drafting, designs, drawings and models. The design in Figure 2 shows the circular micro-strip patch antenna.

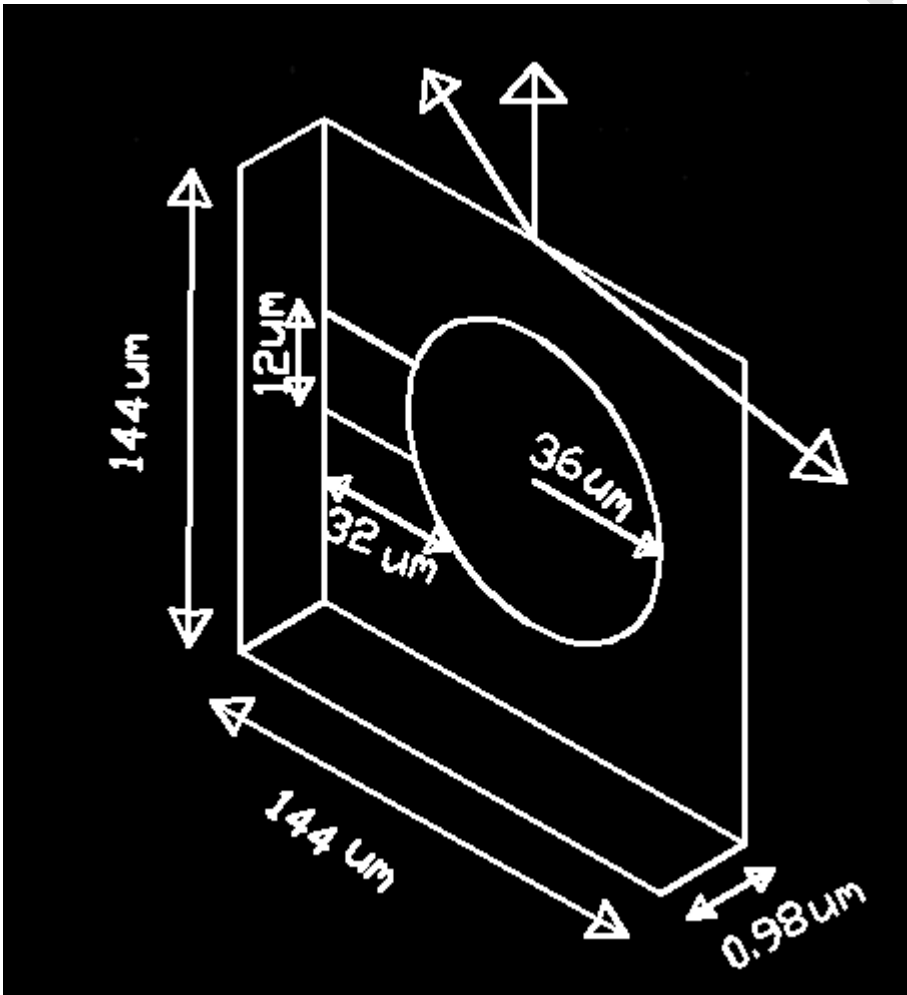


Fig. 2: The proposed Circular Micro-strip Patch Antenna

The Maplesoftware which is a computer algebra system (CAS) that specializes in symbolic mathematics and mathematical modeling was used to calculate the dimension of the micro-strip antenna element as shown in Fig. 2. The parameters of the antenna are calculated based on antenna theory. In the design, the specified parameters are the dielectric constant (ϵ_q) of the substrate, the height of the substrate (s) and the reference frequency (f), RT/Duroid 5880 substrate with dielectric constant of 2.2 was used and substrate height (thickness) was assumed to be $0.98\mu\text{m}$. For mobile communications at terahertz band, the international telecommunication union of Radio-communication (ITU-R) sector recommended 0.3THz to 3THz frequency range as a main part of terahertz based mobile/cellular communications.. The parameters of the circular micro-strip patch antenna are calculated using the following expression as given by [14] and [12].

$$\text{The reference frequency of CMPA, } f = \frac{f_1 + f_2}{2} \quad (1)$$

$$\text{Where } f_1 = 0.3\text{THz}$$

$$f_2 = 3.0\text{THz}$$

Substituting the values of f_1 and f_2 , the reference frequency is given as follows:

$$f = \frac{0.3 + 3.0}{2}$$

$$f = \frac{33}{2} = 1.65\text{THz}$$

$$f = 1.65\text{THz}$$

Hence, the frequency of operation of this design was chosen as 1.65THz.

For fringes where the patch appears electrically large, a length correction factor (R_e) was used as the effective radius.

The effective radius of the circular patch is computed as reported by [12];

$$R_e = \frac{8.791 \times 10^9}{f \sqrt{\epsilon_q}} \quad (2)$$

Where $\epsilon_q = 2.2$ (Dielectric constant)

$f = 1.65\text{THz}$ (Reference frequency)

Putting in the values of ϵ_q and f , the effective radius is;

$$R_e = \frac{8.791 \times 10^9}{1.65 \times 10^{12} \sqrt{2.2}}$$

$$R_e = \frac{8.791 \times 10^9}{1.65 \times 10^{12} \times 1.483239697}$$

$$R_e = \frac{8.791 \times 10^9}{2.4473455 \times 10^{12}}$$

$$R_e = 0.003592055$$

$$R_e = 0.0036\text{cm}$$

$$R_e = 36\mu\text{m}$$

The circular patch radius is given as reported by [15];

$$R = \frac{R_e}{\left\{1 + \frac{2s}{3.142 R_e (\epsilon_q)} \left[\ln \left(\frac{3.142 R_e}{2s} \right) + 1.8 \right] \right\}^{0.5}} \quad (3)$$

Where $\epsilon_q = 2.2$ (Dielectric constant)

$s = 0.98\mu\text{m}$ (Substrate height)

$R_e = 36\mu\text{m}$ (Effective radius)

Substituting the values of ϵ_q , s , and R_e , the radius of the patch is as follows:

$$R = \frac{36\mu\text{m}}{\left\{1 + \frac{2 \times 0.98\mu\text{m}}{3.142 \times 36\mu\text{m} \times 2.2} \left[\ln \left(\frac{3.142 \times 36\mu\text{m}}{2 \times 0.98\mu\text{m}} \right) + 1.8 \right] \right\}^{0.5}}$$

$$R = \frac{36\mu\text{m}}{\left\{1 + \frac{1.96\mu\text{m}}{248.8464\mu\text{m}} \left[\ln \left(\frac{113.112\mu\text{m}}{1.96\mu\text{m}} \right) + 1.8 \right] \right\}^{0.5}}$$

$$R = \frac{36\mu\text{m}}{\left\{1 + 0.007876344 \left[\ln(57.71020408) + 1.8 \right] \right\}^{0.5}}$$

$$R = \frac{36\mu m}{\{1 + 0.007876344[4.055434005 + 1.8]\}^{0.5}}$$

$$R = \frac{36\mu m}{\{1 + 0.007876344[5.855434005 + 1.8]\}^{0.5}}$$

$$R = \frac{36\mu m}{\{1 + 0.046119412\}^{0.5}}$$

$$R = \frac{36\mu m}{\sqrt{1.046119412}}$$

$$R = 35.12 = 35\mu m$$

Length of substrate (Ls) = Length of ground plane (Lg) = 4R_e = 4×36 = 144μm

Width of substrate (Ws) = Width of ground plane (Wg) = 4R_e = 4×36 = 144μm

From the above computations, the effective radius of the circular patch is 36μm and the dielectric material is RT/Duroid 5880 having relative permittivity of 2.2 and loss tangent of 0.0009. The substrate thickness is 0.98μm. The dimension of the ground plane which is at the bottom of the substrate is 144μm × 144μm. The micro-strip feed line dimensions are very important in CMPA to avoid mismatch and ensure maximum power transfer from the source to the load. The quarter wave matching stub method was applied for the feed-line dimensioning. For effective power transfer with the circular patch to achieve the impedance matching of 50Ω between the patch antenna and the transmission line, the dimensions of the micro-strip feed-line are computed as follows.

$$Z_0 = \sqrt{Z_s \times Z_l} \quad (4)$$

Z₀ = Characteristic Impedance,

Z_s = Source Impedance

Z_l = Load Impedance

$$\text{Feed line Width, } W = \frac{(Z_0 \times S)}{(8 \times \epsilon_q)^{0.5}} \quad (5)$$

$$W = \frac{(50 \times 0.98)}{(8 \times 2.2)^{0.5}}$$

$$W = 11.7 = 12\mu\text{m}$$

Effective dielectric constant, ϵ_{eff} is given as reported by [16];

$$\epsilon_{\text{eff}} = \frac{(\epsilon_q + 1)}{2} + \left(\frac{(\epsilon_q - 1)}{2}\right) \times \left(1 + \frac{12S}{W}\right)^{-0.5} \quad (6)$$

$$\epsilon_{\text{eff}} = \frac{(2.2 + 1)}{2} + \left(\frac{(2.2 - 1)}{2}\right) \times \left(1 + \frac{12 \times 0.98}{12}\right)^{-0.5}$$

$$\epsilon_{\text{eff}} = \frac{(3.2)}{2} + \left(\frac{(1.2)}{2}\right) \times \left(1 + \frac{11.7}{11.7}\right)^{-0.5} = 2.02$$

$$\epsilon_{\text{eff}} = 2.02$$

$$\text{Effective wavelength, } \lambda_{\text{eff}} = \frac{\lambda}{\sqrt{\epsilon_{\text{eff}}}} \quad (7)$$

$$\text{But } \lambda = \frac{c}{f}$$

Where c = Speed of light in free space.

λ = Wavelength equivalent of the reference frequency

$$\lambda = \frac{3.0 \times 10^8}{1.65 \times 10^{12}} = 180 \mu\text{m}$$

$$\lambda = 180 \mu\text{m}$$

$$\text{Therefore, } \lambda_{\text{eff}} = \frac{\lambda}{\sqrt{\epsilon_{\text{eff}}}}$$

$$\lambda_{\text{eff}} = \frac{180 \mu\text{m}}{\sqrt{2.02}}$$

$$\lambda_{\text{eff}} = 126.65 \mu\text{m}$$

Feed line Length is given as follows;

$$L = \frac{\lambda_{\text{eff}}}{4} \quad (8)$$

$$L = \frac{126.6 \mu\text{m}}{4}$$

$$L = 31.7 = 32 \mu\text{m}$$

The detailed dimension of the proposed work is shown in Table 1.

Table 1: Design parameters of circular micro-strip patch antenna and their values

Parameters	Values
Reference Frequency (f)	1.65GHz
Effective Radius of the circular patch(R_e)	36 μ m
Substrate Width (W_s) = Ground plane width (W_g)	144 μ m
Substrate Length (L_s)= Ground plane Length (L_g)	144 μ m
Substrate height (s)	0.98 μ m
Width of Micro-strip feed line(W)	12 μ m
Length of Micro-strip feedline (L)	32 μ m

2.2.4 Choice of Antenna Array

The Chebyshev Antenna Array (CAA) design method was chosen for this work in order to minimize the side lobe and to achieve controlled side lobe levels while maintaining a high level of directivity in the desired direction by adjusting the amplitude and phases of the individual antenna elements in the array. Antenna feeding is provided using a feed-line that connects the external edge feed on the dielectric substrate with the conductive patch [17]. In this work, the Chebyshev Antenna Array (CAA) is edge – feed to the radiating patch. This means that the antenna array is placed along the edge of the circular patch antenna. The individual antenna elements are feed from the edge or side of the array rather than from the centre. In this configuration, the feed line is connected to the Circular Micro-strip Patch Antenna (CMPA) at the edge, and the signals are distributed to the elements from the edges of the array. This is to provide a directional radiation pattern with high directivity and gain in a specific direction. Edge – feed antenna arrays offer several advantages over other types of array configurations. One advantage is that they provide wide bandwidth and higher efficiency compared to centre – feed antenna arrays. The best pattern null is achieved by controlling both the amplitude and the phase of each element in the array, as it provides more freedom for the solution space than controlling only the amplitude. Another significant advantage of edge – feed antenna arrays is their ability to achieve beam steering and beam shaping. Azimuthal directional beam steering is obtained by controlling the phase front through a grafting antenna array [18]. In this work, by adjusting the phase and the amplitude distribution of the signals feed to each

element, the antenna array can steer the main beam in a desired direction or shape the radiation pattern to meet specific requirements.

2. 2. 5 Dolph Chebyshev Antenna Array (CAA) Design

The Chebyshev Antenna Array (CAA) design method requires determining the element spacing, amplitude and phase distributions to achieve the desired radiation pattern. This involves estimating the voltage proportion in decibel, calculating the voltage proportion not in decibel, computing the array order, determining the ratio of the chebyshev polynomial function logic (h) to the trigonometry logic $((\sec \delta)^{-1})$, selecting and expanding the required array factor, finding the array amplitude distribution and finally writing out the array factor for phase distribution, $\omega = 0^\circ$ to 180° . In this work, eight (8) array elements with element spacing of 0.5λ was considered to avoid grating lobes

The normalized array factor of an even $(2N) -$ elements, linear array having uniform element spacing and non-uniform amplitude as given by [14] is expressed as;

$$W_{(2 \times N)} = \sum_{u=1}^N t_u \left(\frac{\sec[\{2(u-0.5)\}\delta]^{-1}}{\cos[\ln(e^N \times e^{-N})]} \right) \quad (9)$$

While for odd $(2N+1) -$ elements is given in Equation 10.

$$W_{(2 \times N)+1} = \sum_{u=1}^{N+1} t_u \left(\frac{\sec[\{2(u-0.5)\}\delta]^{-1}}{\cos[\ln(e^{(N+1)} \times e^{-(N+1)})]} \right) \quad (10)$$

Where $\delta = \pi S / \lambda \cos(\omega)$,

t_u = Array amplitude distribution and

S = Inter-element spacing ($S = 0.5\lambda$ for this work).

Expanding equation 9 for eight (2×4) elements to avoid grating lobes, yields Equation 11.

$$W_{(2 \times 4)} = t_1 \left(\frac{\sec[\{2(u-0.5)\}\delta]^{-1}}{\cos[\ln(e^4 \times e^{-4})]} \right) + t_2 \left(\frac{\sec[\{2(u-0.5)\}\delta]^{-1}}{\cos[\ln(e^4 \times e^{-4})]} \right) + t_3 \left(\frac{\sec[\{2(u-0.5)\}\delta]^{-1}}{\cos[\ln(e^4 \times e^{-4})]} \right) + t_4 \left(\frac{\sec[\{2(u-0.5)\}\delta]^{-1}}{\cos[\ln(e^4 \times e^{-4})]} \right) \quad (11)$$

Dolph chebyshev antenna array polynomial of order q (the order is one less than the total number of element, that is $q = M-1$) for inter-element spacing of half wavelength is determined using recursive formula given by [14, 19] and is expressed as follows;

$$A_{(q\lambda/2S)}(h) = 2hA_{(q\lambda/2S)-1}(h) - A_{(q\lambda/2S)-2}(h) \quad (12)$$

For the following conditions

1. When $h > 1$, $A_{(q\lambda/2S)}(h) = \cosh(qsech(h))$
2. If $h < -1$, $A_{(q\lambda/2S)}(h) = (-1)^q \cosh(qsech(h))$
3. As $-1 < h < 1$, $A_{(q\lambda/2S)}(h) = \cos(qsec(h))$

The polynomial functions for the antenna array design are shown in table 2 while $(\sec q\delta)^{-1}$ (where $\delta = 00$ to 07) are obtained by substituting $(h = (\sec \delta)^{-1})$ in each row of $A_{(q\lambda/2S)}(h)$ in table 2a or by using Binomial theorem and Euler's formular which is the combination of trigonometry function and complex number .

For example, when $q = 03$, $(\sec 3\delta)^{-1} = (\sec \delta)^{-1} = 4((\sec \delta)^{-1})^3 - 3(\sec \delta)^{-1}$

That is, using Euler's formular, $(\sec 3\delta)^{-1} = (\sec \delta)^{-1} + j \sin 3\delta$

Applying binomial theorem to the above expression

$$(\sec 3\delta)^{-1} = ((\sec \delta)^{-1} + j \sin \delta)^3$$

Let $D = (\sec \delta)^{-1}$, $C = \sin \delta$

Therefore,

$$(\sec 3\delta)^{-1} = (D + jC)^3$$

Using the Pascal triangle in table 2b

$$(\sec 3\delta)^{-1} = D^3 + 3D^2(jC) + 3D(jC)^2 + (jC)^3$$

$$(\sec 3\delta)^{-1} = D^3 + 3D^2(jC) - 3D C^2 + (jC)^3$$

$$(\sec 3\delta)^{-1} = D^3 - 3D C^2$$

$$(j \sin \delta) = D^2(jC) + (jC)^3$$

Substituting $\sin^2 \delta = 1 - (\sec^2 \delta)^{-1}$ or $C^2 = 1 - D^2$

Therefore, $(\sec 3\delta)^{-1} = D^3 - 3D(1 - D^2)$

$$(\sec 3\delta)^{-1} = D^3 - 3D + 3D^3$$

$$(\sec 3\delta)^{-1} = D^3 + 3D^3 - 3D$$

$$(\sec 3\delta)^{-1} = 4D^3 - 3D$$

Recall that $D = (\sec \delta)^{-1}$

Hence,
$$(\sec 3\delta)^{-1} = 4((\sec \delta)^{-1})^3 - 3(\sec \delta)^{-1}$$

Applying the same principle, $(\sec 5\delta)^{-1}$ and $(\sec 7\delta)^{-1}$ are computed as follows;

$$(\sec 5\delta)^{-1} = 16((\sec \delta)^{-1})^5 - 20((\sec \delta)^{-1})^3 + 5(\sec \delta)^{-1}$$

$$(\sec 7\delta)^{-1} = 64((\sec \delta)^{-1})^7 - 112((\sec \delta)^{-1})^5 + 56((\sec \delta)^{-1})^3 - 7(\sec \delta)^{-1}$$

Table 2a: The Chebyshev polynomial functions for the Antenna array design. **Table 2b:** Pascal triangle for array of M-Elements.

q	$A_{(q\lambda/2s)}(h)$
00	1
01	h
02	$2h^2 - 1$
03	$4h^3 - 3h$
04	$8h^4 - 8h^2 + 1$
05	$16h^5 - 20h^3 + 5h$
06	$32h^6 - 48h^4 + 18h^2 - 1$
07	$64h^7 - 112h^5 + 56h^3 - 7h$

M	Pascal Triangle
0	1
1	1 1
2	1 2 1
3	1 3 3 1
4	1 4 6 4 1

Using voltage proportion of 26dB, the proportion not in decibel is calculated as reported by [20];

$$A_{(q\lambda/2S)}(K_0) = 10^{\frac{26\text{dB}}{20}} = 20.$$

Where K_0 is the ratio of the chebyshev polynomial function logic (h) to the trigonometry logic $((\sec \delta)^{-1})$ for $A_{(q\lambda/2S)} > 1$, $K_0 > 1$

Array order, $q = (M - 1) = 8 - 1 = 7$ and $S = 0.5\lambda$

$$\text{Therefore, } A_{(7\lambda/2S)}(K_0) = (M - 1)\text{sech}(K_0) = \ln\left(K + \sqrt{K^2 - 1}\right)$$

$$= 7\text{sech}(K_0) = \ln\left(20 + \sqrt{20^2 - 1}\right)$$

$$= 7\text{sech}(K_0) = \ln\left(20 + \sqrt{400 - 1}\right)$$

$$7\text{sech}(K_0) = 3.69$$

$$\text{sech}(K_0) = \frac{3.69}{7}$$

$$\text{sech}(K_0) = 0.527$$

$$\text{Hence, } K_0 = \text{sech}^{-1}(0.527) = 1.142$$

Using Equation 11, the array amplitude distribution for eight (2×4) elements chebyshev arrays are computed as follows;

$$W_{(2 \times 4)} = t_1 \left(\frac{(\sec \delta)^{-1}}{\cos\left(\frac{1}{2} \ln(e^4 \times e^{-4})\right)} \right) + t_2 \left(\frac{(\sec 3\delta)^{-1}}{\cos\left(\frac{1}{2} \ln(e^4 \times e^{-4})\right)} \right) + t_3 \left(\frac{(\sec 5\delta)^{-1}}{\cos\left(\frac{1}{2} \ln(e^4 \times e^{-4})\right)} \right) +$$

$$t_4 \left(\frac{(\sec 7\delta)^{-1}}{\cos\left(\frac{1}{2} \ln(e^4 \times e^{-4})\right)} \right) =$$

$$\left(\frac{1}{\cos\left(\frac{1}{2} \ln(e^4 \times e^{-4})\right)} \right) [t_1 (\sec \delta)^{-1} + t_2 [4((\sec \delta)^{-1})^3 - 3(\sec \delta)^{-1}] + t_3 [16((\sec \delta)^{-1})^5 - 20((\sec \delta)^{-1})^3 + 5\sec \delta - 1] + t_4 [64\sec \delta - 17 - 112\sec \delta - 15 + 56\sec \delta - 13 - 7\sec \delta - 1]$$

$$= \left(\frac{1}{\cos\left(\frac{1}{2} \ln(e^4 \times e^{-4})\right)} \right) [(\sec \delta)^{-1} [t_1 - 3t_2 + 5t_3 - 7t_4] + ((\sec \delta)^{-1})^3 [4t_2 - 20t_3 + 56t_4] +$$

$$\sec \delta - 1516t_3 - 112t_4 + \sec \delta - 1764t_4 = A_{7\lambda/2S}(h), s = 0.5\lambda.$$

Substituting $(\sec \delta)^{-1} = \frac{h}{K_0}$, this is the relationship between the trigonometry logic $((\sec \delta)^{-1})$ and the chebyshev polynomial function logic (h).

$$= \left(\frac{1}{\cos(\ln(e^4 \times e^{-4}))} \right) \left[\frac{h}{(K_0)} [t_1 - 3t_2 + 5t_3 - 7t_4] + \frac{h^3}{(K_0)^3} [4t_2 - 20t_3 + 56t_4] + \frac{h^5}{(K_0)^5} [16t_3 - 112t_4] + \frac{h^7}{(K_0)^7} [64t_4] \right]$$

Comparing the power term of each to find the amplitude distribution starting from the highest power term.

For power seven

$$\frac{h^7}{\cos(\ln(e^4 \times e^{-4})) (K_0)^7} [64t_4] = (64)h^7$$

$$64h^7 t_4 = 64h^7 \cos(\ln(e^4 \times e^{-4})) (K_0)^7$$

$$t_4 = \cos(\ln(e^4 \times e^{-4})) (1.142)^7 = 2.533160617$$

For power five

$$\frac{h^5}{\cos(\ln(e^4 \times e^{-4})) (K_0)^5} [16t_3 - 112t_4] = (-112)h^5$$

$$h^5 [16t_3 - 112t_4] = (-112) \cos(\ln(e^4 \times e^{-4})) (K_0)^5 h^5$$

$$h^5 [16t_3 - 112t_4] = (-112) \cos(\ln(e^4 \times e^{-4})) (1.142)^5 h^5$$

$$16t_3 - 112(2.533160617) = -217.5447176$$

$$16t_3 - 283.7139891 = -217.5778557$$

$$16t_3 = -217.5778557 + 283.7139891$$

$$t_3 = \frac{66.16927152}{16} = 4.13557947$$

For power three

$$\frac{h^3}{\cos(\ln(e^4 \times e^{-4})) (K_0)^3} [4t_2 - 20t_3 + 56t_4] = (56)h^3$$

$$h^3[4t_2 - 20t_3 + 56t_4] = (56)\cos(\ln(e^4 \times e^{-4}))(K_0)^3h^3$$

$$h^3[4t_2 - 20t_3 + 56t_4] = (56)\cos(\ln(e^4 \times e^{-4}))(1.142)^3h^3$$

$$4t_2 - 20(4.13557947) + 56(2.533160617) = 83.41660088$$

$$4t_2 - 82.7115894 + 141.8569946 = 83.40389613$$

$$4t_2 = 83.40389613 + 82.7115894 - 141.8569946$$

$$t_2 = \frac{24.25849093}{4} = 6.064622732$$

For power one

$$\frac{h}{\cos(\ln(e^4 \times e^{-4}))(K_0)} [t_1 - 3t_2 + 5t_3 - 7t_4] = (-7)h$$

$$h[t_1 - 3t_2 + 5t_3 - 7t_4] = (-7)\cos(\ln(e^4 \times e^{-4}))(K_0)h$$

$$h[t_1 - 3t_2 + 5t_3 - 7t_4] = (-7)\cos(\ln(e^4 \times e^{-4}))(1.142)h$$

$$t_1 - 3(6.064622732) + 5(4.13557947) - 7(2.533160617) = -7.994$$

$$t_1 - 18.1938682 + 20.67789735 - 17.73212432 = -7.994$$

$$t_1 = -7.994 + 18.1938682 - 20.67789735 + 17.73212432 =$$

$$t_1 = 7.254095166$$

Dividing each amplitude distribution by $t_4 = 2.533160617$, therefore, the array amplitude distribution for eight (2×4) elements chebyshev arrays are $t_1 = 2.86$, $t_2 = 2.39$, $t_3 = 1.63$, and $t_4 = 1.00$.

The directivity of dolph chebyshev array (D_{DCA}) from equation 11 is expressed as follows;

$$D_{DCA} = 2 \left\{ \frac{(t_1 + t_2 + t_3 + t_4)^2}{[(t_1)^2 + (t_2)^2 + (t_3)^2 + (t_4)^2]} \right\} \quad (13)$$

The directivity in decibel of the dolph chebyshev antenna array used in this work is expressed in equation 14 as reported by [14];

$$D_{DCA} (dB) = \log_{10} \frac{D_{DCA}}{10} \quad (14)$$

As the Chebyshev Antenna Array (CAA) is edge – feed to the Circular Micro-strip Patch Antenna (CMPA), by proper adjustment of the phase or directional angle and the amplitude distribution, the antenna steered the main beam in a desired direction and shaped the radiation pattern as required

3.Results and Discussion

3.1. Results and Analysis

3.1.1 Data Presentation and Analysis

In this section, a summary of the data obtained for this investigation are analyzed and presented. With the aid of Maple software and 2D data plotter, these values are obtained, plotted and compared graphically.

3.1.1.1 Antenna Radiation Pattern Factors

As the complexity of equations is beyond human handling limits, a useful practical way to get the symbolic (sample) results is through Maple software to perform the symbolic (sample) computations and get the sample results [21].

In this work, the Chebyshev Antenna Array (CAA) is edge – feed to the Circular Micro-strip Patch Antenna (CMPA), focusing on adjusting both the amplitude distribution and the phase for the antenna array factor. Due to the complex nature of the antenna array models, Maple software was chosen as the most effective practical approach to adjust both the amplitude distribution and the phase for steering/directional angles (ϕ) within the range of 0° to 180° at 30° intervals and a frequency of 1.65THz. The software was employed to conduct sample computations, and the resulting data is presented in Table 3. By this adjustment, the antenna steered the main beam in a desired direction and shaped the radiation pattern as required in figure 3.

Table 3: Antenna array factors and the corresponding directional azimuth angles, ϕ .

Angle, ϕ	0°	30°	60°	90°	120°	150°	180°
Array factor (dB)	7.84	7.85	7.87	7.88	7.87	7.85	7.84

The dependent variable is the array factor while the independent variable is the directional angle.

3.1.1.2 The stability of the antenna radiation pattern

To determine the stability of the radiation pattern and to provide answer to the research questions, Pearson Correlation is applied to test for the relationship between the two variables (antenna array factor and directional angle) of the antenna radiation pattern as shown in Table 4.

Table 4:The Antenna radiation pattern Pearson Correlation

S/N	X	Y	X - \bar{X}	Y - \bar{Y}	(X - \bar{X}) ²	(Y - \bar{Y}) ²	(X - \bar{X})(Y - \bar{Y})
1.	0	7.84000	-90	-0.01714	8100	0.00029	1.5426
2.	30	7.85000	-60	-0.00714	3600	0.00005	0.4284
3.	60	7.87000	-30	0.01286	900	0.00017	-0.3858
4.	90	7.88000	0	0.02286	0	0.00052	0
5.	120	7.87000	30	0.01286	900	0.00017	0.3858
6.	150	7.85000	60	-0.00714	3600	0.00005	-0.4284
7.	180	7.84000	90	-0.01714	8100	0.00029	-1.5426
Tota l	360	55			25200	0.00154	0

Pearson Coefficient Correlation (P) is the ratio of the sample covariance between the two variables to the product of their sample standard deviations as expressed in Equation 15.

$$P = \frac{\sum((X - \bar{X})(Y - \bar{Y}))}{\sqrt{\sum(X - \bar{X})^2 \times \sum(Y - \bar{Y})^2}} \quad (15)$$

Where

P = Pearson Correlation Coefficient

X = X (angle in degree), – variable values

Y = Y (array factor in dB) – variable values

\bar{X} = Mean of X variable values (=90)

\bar{Y} = Mean of Y variable values (=7.85714)

$$P = \frac{0}{\sqrt{(25200)(0.00154)}}, \quad P = 0$$

Since P = 0, there is zero correlation between the variables, meaning there is no linear relationship between the two variables. Applying Chi- Square hypothesis test for the stability of the radiation pattern formed by the two variables, as shown in Fig. 3 and Table 5 respectively for the radiation pattern stability determination

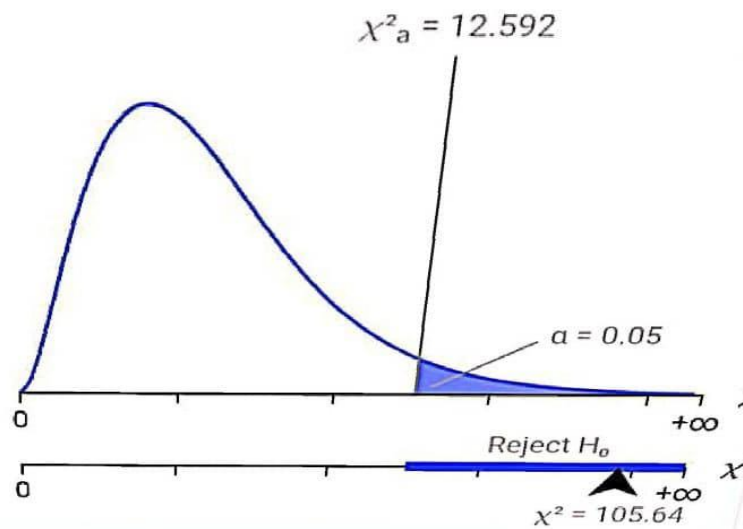


Fig. 3: Chi-Square Hypothesis Plot

Null hypothesis, H_0 (The radiation pattern is not stable)

Alternate or research hypothesis, H_a (The radiation pattern is stable).

For $P \leq \alpha$, Reject H_0

Table 5: Radiation pattern Hypothesis Test Results

Level of significance (α)	Critical Value	Test Statistic	P-value	Rejection Region	Decision
$\alpha = 0.05$	$X_{\alpha}^2 = 12.592$	$X^2 = 105.64$	0.000	$X^2 > X_{\alpha}^2$	$P \leq \alpha$, Reject H_0 at $\alpha = 0.05$

For the stability of the antenna radiation pattern, Table 5 shows that the radiation pattern is stable and there is a significant difference or relationship between the antenna array factor and the directional angle to form a perfectly antenna radiation pattern of low side lobe level, appreciable beam width and high directivity. They are not linearly related but non-linearly related.

3.1.1.3 Impedance matching

In the antenna design, perfect transfer of signal from the source to the load impedances is very necessary and this is achieved with a characteristic impedance of 50Ω to ensure maximum power transfer from the source to

the load which gives unity Voltage Standing Wave Ratio (VSWR) as shown in Fig. 4. This is to avoid mismatch, signal loss and distortion.

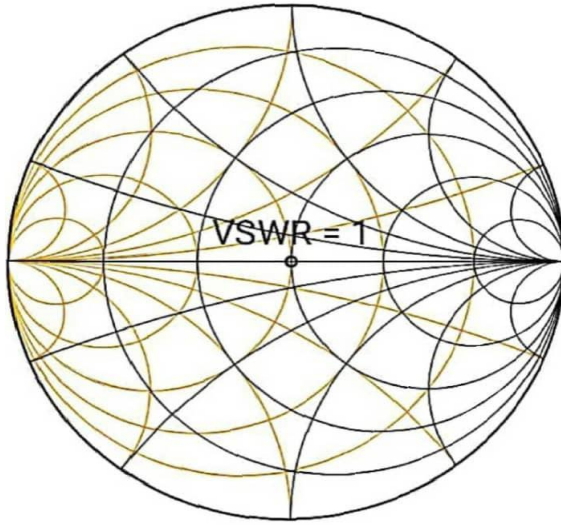


Fig.4: Smith Chart of the Impedance Matching

$$\begin{aligned} \text{Return loss} &= 20\text{Log}_{10}^{\text{VSWR}} && (16) \\ &= 20\text{Log}_{10}^1 = 0 \end{aligned}$$

3.1.1.4 Antenna radiation pattern

In context of antenna radiation pattern, a pointed curve of Fig. 5 refers to the shape of the radiation pattern produced by the antenna. A radiation pattern represents the distribution of radiated power in different directions from the antenna. A pointed curve indicates that majority of the radiated power is concentrated in a specific direction compared to others. That means that the antenna is more focused and has a narrower beam width in association with the pointed curve

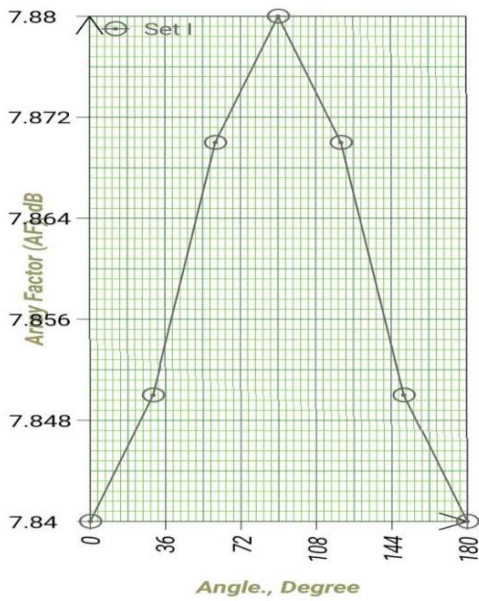


Fig. 5: Graphical Representation of the Antenna Radiation Pattern

3.1.1.5 Half Power Beam Width (HPBW) and First Null Beam Width (FNBW)

The HPBW is the angle formed by two lines in the polar plot extending from the center of the curve to the 3-dB drop or down points. In Fig. 6, the Half Power Beam Width (HPBW) is 30° which is the angular separation in which the magnitude of the radiation pattern decrease by 3-dB from the peak of the main beam. It is the measure of the beam width between the points on either side of the main lobe where the power drops to half its maximum value and is use to describe the directivity of the antenna. The First Null Beam Width (FNBW) is twice HPBW. It is the annular separation between the first nulls of the radiation pattern or the main lobe where the signal strength falls to zero for the first time. The First Null Beam Width (FNBW) is 60° .

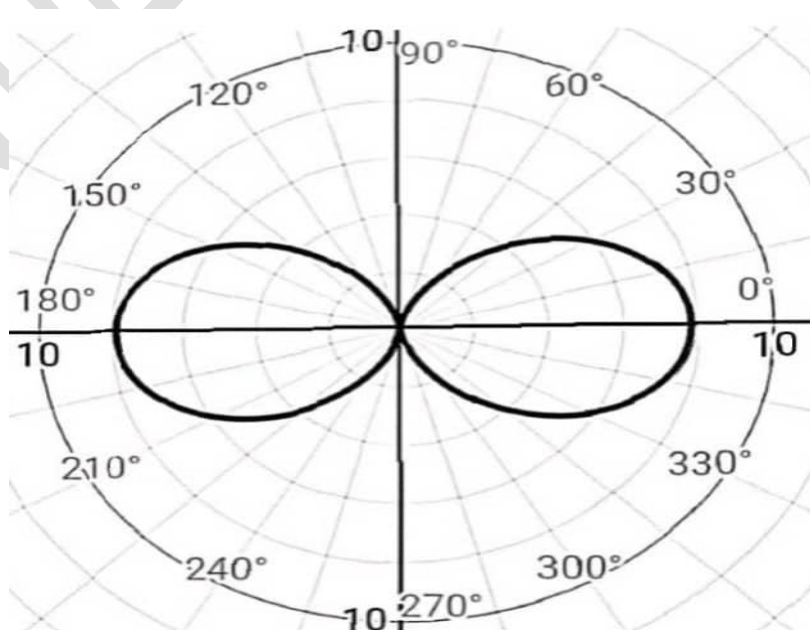


Fig. 6: The polar plot of the Antenna Radiation Pattern in the Azimuth Angle of 0° and 180° .

3.1.1.6 Main lobe, side lobe and side lobe level

In the antenna radiation pattern, the main lobe, side lobe and side lobe level refers to certain characteristics of the radiation pattern. Main lobe is the region in the radiation pattern of an antenna or directional signal where the majority of the antenna's radiation is concentrated. It represents the primary direction in which the antenna radiates or receives the strongest signal. Side lobes are additional lobes or unwanted signal that appears in the radiation pattern of an antenna other than the main lobe. They are usually smaller in magnitude compared to the main lobe and are located in directions away from the main lobe. The goal of this work is to eliminate or minimize side or minor lobes to put more power into the major lobe. Side lobe level is a measure of magnitude or power of the side lobes relative to the main lobe. It represents the level of energy radiated or received in the side lobes compared to the major or main lobe. In other words, it is the length between the main lobe and the side lobe closer to the main lobe. A lower side lobe level indicates a more focused and directional radiation pattern while a higher one indicate more energy is radiated or received in directions other than the main lobe. Side lobe level is used to quantify the performance of an antenna or smart signal processing system, in terms of its ability to suppress unwanted radiation or interference in directions other than the desired main lobe direction. To minimize interference from unwanted directions, it is beneficial to have lower side lobe levels (SLL) in mobile communication[22].

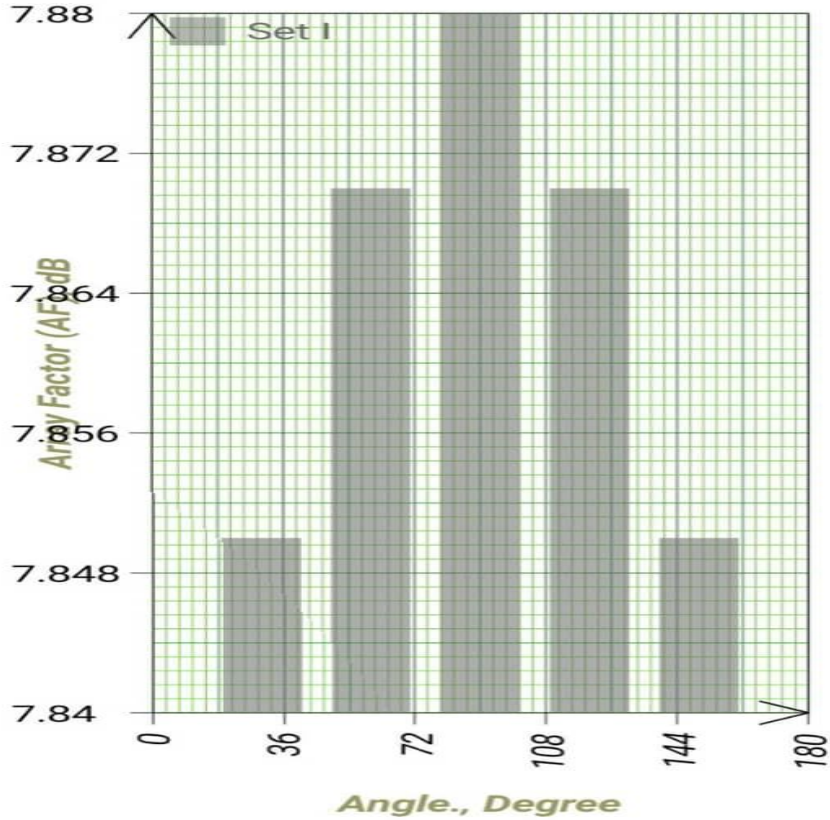


Fig. 7: Bar Chart Representation of the Antenna Radiation Pattern

In Fig. 7, the main lobe occurs at directional angle of 90° , while side lobes occur at angle 30° , 60° , 120° , and 150° , respectively and at angle 0° and 180° , the side lobe is at the directional angle axis. The side lobe level which is the difference between the main lobe and the first side lobe near the main lobe is measured as 0.01dB in Fig. 7.

3.1.1.7 Antenna Directivity

The 3D plane plot of the antenna's directivity is shown in Fig. 8. The directivity of the antenna is approximately equal to 9dB with no energy leakage in the undesired directions which indicate its ability to concentrate the radiated power in a specific direction.

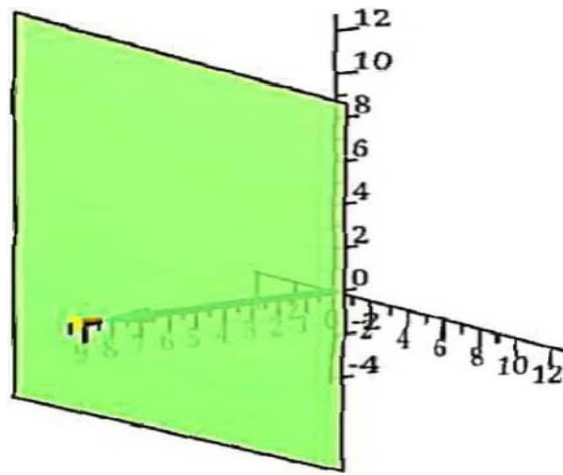


Fig. 8: The 3D Directivity plane Plot

The low side lobe level of 0.01dB for a circular micro-strip patch antenna with eight (8) elements and separation distance of 0.5λ and directivity of 9dB is relatively desirable for mobile communication because it indicates better control over the radiation pattern which can result in improved signal strength and reduced interference with neighboring antennas. This can lead to better overall performance, greater connectivity and reliability of the mobile communication system.

3.2 Discussion

Fig. 7 shows the antenna's radiation pattern which exhibits a low side lobe level of 0.01dB, indicating a focused beam with minimal or no energy leak in undesired directions. This antenna characteristic is crucial for minimizing interference, improving reliability and maximizing signal strength in mobile communication systems. Furthermore, the antenna demonstrated a high directivity and gain of approximately 9dB as shown in Fig. 8, indicating its ability to concentrate the radiated power in a specific direction. This high directivity is beneficial for achieving broader coverage area and improving the overall performance of the communication system serving mobile users.

Fig. 6 shows that the antenna has a HPBW of 30° thereby providing a reasonably wide coverage area. This feature is advantageous for accommodating multiple users simultaneously within the base stations coverage zone. Similarly, the FNBW of 60° indicates the ability of the antenna array to nullify signals within wider angular range. This capability is important for reducing interference from adjacent channels or unwanted signals leading to improved signal quality, clearer and more reliable communication environment in mobile communication system.

Additionally, the results from this study demonstrate that the following benefits of Circular Micro-strip Patch Antenna (CMPA) can be achieved. And they are; compact size, low cost, greater bandwidth, low profile, ease of integration with other Electronic components and systems.

Therefore, the contribution of this work in developing antenna with these characteristics hold great promise for more efficient, reliable and high performance mobile communication systems, benefiting both service providers and end users.

3.3 Comparison with other studies

Table 6: This Study versus Previous Studies

Parameters	This Study	[12]	[16]
Frequency	1650GHz	5.5 GHz	7.4 – 12GHz
Directivity	9.0dB	4.28dBi	-
Gain	9.0dB	3.23dB	3dB
Side lobe level	0.01dB	-	17.71dB

Table 6 shows that this study generated a better results than previous studies because the higher the frequency, directivity and gain the better the antenna performance. Also the lower the side lobe level the better the interference reduction. Thus, it is recommendation for “large commercial production for the benefit of mankind”

3.4 Challenges encountered

In the course of carrying out the work, challenges were encountered such as the unavailability of the needed software for stimulation which was also overcome by using alternative software (Maple software). It is a computer algebra system like Matlab and a valuable tool in antenna design and analysis capabilities to Researchers, Engineers and Students. It is a popular choice among researchers and professionals in the STEM (Science, Technology, Engineering, and Mathematics) fields,

3.5 Future Study

It is necessary to consider integrating advanced signal processing techniques such as beamforming and adaptive algorithms to further enhance the antenna’s performance. Additionally, the designed antenna and array can necessarily be validated for its effectiveness in real-world scenario. Furthermore, it is worth nothing that at very high frequency of terahertz range, feed line design becomes more challenging due to factors like signal losses,

dispersion and interference. Therefore, it is recommended to do proper dimensioning of the micro-strip feed line to ensure accurate impedance matching and optimal performance for any specific application.

4. Conclusion

The design of a circular micro-strip patch antenna, at tetrahertz frequency range with the incorporation of chebyshev antenna array for improved directivity and gain of mobile communication base station has been the crux of this work. Analysis of the design showed that the antenna's radiation pattern exhibits a low side lobe level of 0.01dB, indicating a focused beam with minimal or no energy leak in undesired directions. This distinguishing feature is significant for interference reduction and signal strength maximization in mobile communication systems. Additionally, the antenna established a high directivity and gain of approximately 9dB, which indicate its ability to centre the radiated power in a particular direction. This high directivity is good for achieving extended coverage area and improvement of the overall performance of the communication system. The HPBW of 30° provides a reasonably wide coverage area, which is helpful in accommodating more than one mobile subscriber simultaneously within the base stations coverage zone. Lastly, the FNBW of 60° showed its capability in reducing interference from neighboring channels or undesirable angle resulting in improved signal quality in mobile communication system. Thus, designed circular micro-strip patch antenna with the incorporated Chebyshev antenna array is suitable for mobile communication applications for improved directivity and gain of mobile base station. Furthermore, the low side lobe level, high directivity and gain as well as the appropriate HPBW and FNBW values make the antenna ideal for improving signal quality, coverage area and minimizing interference. With these promising results, and potential for further enhancements, the designed antenna hold great help for mobile communication system base station.

References

1. Nagma P, Khaizuran A, Kafigual Md, Muhammed A. Performance Analysis of Antenna Diversity Technique with Wavelet Transform using Array Gain for Millimeter Wave Communication. *Electronics*. 2022, 11(16), 2626.
2. Sandeep D. A Review Paper on Smart Antenna for Mobile Communication. *International Journal of Engineering Research and Technology (IJERT)* .2017, VIMPACT Vol. 5, Issue 23, pages1-2. DOI: 10.17577/IJERTCONV51S23014
3. IoWave Inc. Smart Antenna. <http://www.iowave.com/>. March 15, 2022.

4. Soheli Md, Bijoy R, Md K, Tanjil A, Shanriar Md, Mostafizur, R. Bulletin of Electrical Engineering and Informatics, Volume 12, number 4, August, 2023. PP. 2173 -2184.
5. Onu F, Ikoporo S. Comparative Study of Fiber Optic and Wireless Technologies in Internet Connectivity. International Journal of Computer Applications Technology and Research.2016, Volume 5, Issue 6, pp. 403 – 411. ISSN:- 2319 – 8656.
6. Bandewar S, Chauudhary V. Design and Analysis of Smart Antenna for Mobile Application. SAMRIDOHI: A Journal of Physical Sciences, Engineering and Technology, 2023, 15(1). pp. 139 – 147.
7. Soheli MdR, Rahman M. Study of Micro-strip Patch Antenna for Wireless Communication Systems. International Conference for Advancement in Technology (ICONAT) Goa, Indian, 2022.
8. Vivek K, Manju J, Deepak R, Vikas K. Advances in Mobile Communication by Implementation of smart antennas. IJECT, 2013, Vol. 4, Issue 3, Pages 2 - 4.
9. Xinxue L, Xiaoli L, Guan J. Performance Analysis of Directional Antenna for Small Base Station. EITCE '21: Proceedings of the 2021, 5th International Conference on Electronics, Information and Technology, 2021. Pages 287 – 291.
10. Okhaifoh JE, Oko-Oboh AA, Umayah EN. Single Polarized Micro-strip Antenna Design for Mobile Communication Base Station. International Journal of Engineering and Advanced Technology. 2013, Vol. 3, Issue 1, pages 58-61.
11. Pazil A, Rahman N, Ramli N, Razak N. Comparative Analysis on Different Feeding Techniques of Textile Antenna for GPS L1 Application. Journal of E.S.D. Technological Advances, 6(1).2021,PP. 27 - 28.
12. Chaitali, M., Mahfujur, R., and Abu, Z. (2021). Design of a Circular Microstrip Patch Antenna for WLAN Applications. International Journal on AdHoc Networking System (IJANS). 2021, Vol. 11. No. 3, Pages 1-11.
13. Krishanu K, Ankan B, Firdous H, Narendra N. Design and Analysis of a Low-Profile Micro-strip Antenna for 5G Application using AI- Base PSO Approach. Journal of Telecommunications and Information Technology. ARCHIVES, Number 3, 2023
14. Balanis C. Antenna Theory Analysis and Design. 2005
15. Yuliana R, Hepi L, Sardjito. The Characteristic of a 3.5GHz Circular Patch Antenna using Open – Ring Artificial Dielectric. Proceeding of the 2nd International Seminar of Science and Applied Technology (ISSAT). 2021, PP 387-393

16. Bayana L, Chennupall B, Nagendram S, Kalyan S. Design and analysis of Circular Patch Antenna. *Journal of Physics Conference series*. 2020. Doi : 10.1088/1742-6596/1804/1/012200. pp 1 – 7.
17. Nandalal, V., Sathishkumar, N., Manikandam, T., Anandkumar, V., and Indhumathi, G. (2020). Design of Rectangular Micro-strip Patch Antenna with Edge Feeding Technique for Marine Applications. *International Journal of Oceans and Oceanography*. 2020, Volume 14, Number 1, PP. 101 – 108. ISSN 0973-2667
18. Shi Z, Daixin L, Wenlei L, Jingye C, Daoxin D, Yaocheng S. Low Sidelobe Silicon Optical Phased Array with Chebyshev Amplitude Distribution. *Nanophotonics*. 2024, 13(3): PP. 263 – 269.
19. Oluwole A, Srivastava V. Features and Futures of Smart Antennas for Wireless Communication. (A Technical Review). *Journal of Engineering Science and Technology Review*. 2018, 11 (4), pages 8-21.
20. Pradhan H, Mangarj B, Behera S. Chebyshev- based array for beam steering and null. *International Journal of microwave and wireless technologies; Cambridge*. 2022, vol. 14, Issue 2.
21. Wang, Y., Soltani, M., and Hussain, D.M.A. Dynamic Modeling and Simulation of Marine Satellite Tracking Antenna Using Lagrange Method. In *Proceedings of UKSim-AMSS 18 th International Conference on Computer Modeling and Simulation(UKSim)*(PP. 135 – 140). IEEE Press. 2016. <https://doi.org/10.1109/UKSim.2016.64>
22. Anindita K, Jibendu S. *Journal of Telecommunications and Information Technology (JTIT)*. Volume 2024. Number 1, pp. 26 – 32.